



Seismic Fragility of the SMART Tunnel Under Near-Field Earthquakes

Syarifah Salwania Syed Mohd Zin¹⁾, *Nik Zainab Nik Azizan^{*}), Ronal Hamonangan Tua Simbolon²⁾

¹⁾Faculty Of Civil Engineering & Technolog, University Malaysia Perlis
s211203003@studentmail.unimap.edu.my

^{*}Faculty Of Civil Engineering & Technology University Malaysia Perlis
nikzainab@unimap.edu.my

²⁾Faculty Of Civil Engineering, Islamic University Of North Sumatera
ronal.h.tsimbolon@ft.uisu.ac.id

Abstract– This study investigates the seismic performance of the SMART Tunnel under near-field earthquake conditions, with a focus on how tunnel burial depth influences fragility, crack development, and structural response. The research began with a comprehensive literature review to establish a theoretical basis for seismic analysis and soil-structure interaction. Four 2D finite element models representing tunnel depths of 0 m, 5 m, 10 m, and 12.2 m were developed using ABAQUS, with realistic soil and structural properties. Seismic input was obtained from the PEER Ground Motion Database and processed through SeismoSignal to generate acceleration-time histories and response spectra. Time-history analyses were then conducted to simulate tunnel behaviour under selected near-field earthquakes. Key structural responses, such as stress distribution and crack propagation, were analysed to evaluate damages. Fragility curves were developed for each model to assess the probability of damage under varying seismic intensities. The findings show that Model 4, located 12.2 m above the rock layer, performs the best due to its ability to accommodate larger displacements before failure, benefiting from increased flexibility in softer soils. In contrast, Model 1, placed directly on the bedrock, was the least effective, showing early collapse under lower seismic loads. These results emphasise the importance of depth and soil interaction in seismic tunnel design.

Keywords: Load forecasting, Load growth, Electricity consumption

1. INTRODUCTION

Although the occurrence of seismic activity in Southeast Asia is less frequent compared to high seismic regions, its threat is increasing in Malaysia due to its location being too close to the Pacific Ring of Fire, which is the epicentre of more than 90 percent of earthquakes in the world [12]. However, until recently, seismic awareness remained low in Malaysia, and occurrences of incidents like the 2015 Ranau quake in Sabah that was a magnitude 6.0 [11] have drawn attention to the fact that Malaysia is exposed to seismic hazard. This event highlights the idea that although Malaysia is not directly placed on active fault lines, the strength of the earthquakes occurring in adjacent areas such as Indonesia and Philippines may have serious implications, since most of the already-built structures in the country remain inadequately seismically treated [4].

Development of better seismic risk evaluation and reduction is especially relevant in old cities with high population density and outdated infrastructure like George Town, Penang. Literature surveys conducted recently have found that there exists a crucial radar def: cavities in seismic readiness and awareness, particularly among people who live in high-rise buildings along with heritage buildings [2].

Given the easy accessibility of local soil classification data, the initial stage of vulnerability mapping and seismic mitigation plans is becoming more practical in Penang [7]. Another important destructive force of seismic risk is the ground motion characteristics, especially near-fault ground motion that is characterised by the high-intensity and short-duration pulses that have been known to cause major structural damage within the 15–20 km surrounding a fault rupture [15]. The types of such motions can be split into non-pulse, fling-step, and directivity pulse types and cause different seismic responses. It was proved that directivity pulse ground motions lead to the maximum displacement and structural damage owing to the concentrated release of energy.

The dynamics of structures during an earthquake are further affected by various factors, including the type of soil, the depth of the tunnel or structure, and the immediate geological environment, that impact the response, which is generally referred to as the seismic behaviour of a structure [3]. Undertaking these interactions in a systematic fashion has currently led to the development of incremental dynamic analysis (IDA) as a major methodology to assess the seismic behaviour of buildings. IDA exposes a structure to increasingly higher-scaled ground motions until it collapses, which brings about the ability to chart the generated IDA curves that signify a correlation between the ground movement level and how it responds.

The approach is quite useful for addressing underground buildings and infrastructures, where the performance of soil-structure interaction and the near-field characteristics of ground motions are both highly challenging and essential [10]. The fragility curve is another crucial instrument utilised in the estimation of the likelihood of a structure reaching or surpassing established damage levels at numerous scales of seismic strength [9]. Fragility curves are extensively used in bridge and fragility assessments of dams, tunnels, and other critical infrastructure.



2. METHODOLOGY

To determine seismic performance through finite element modelling in this study, the SMART Tunnel in Kuala Lumpur is adopted as the case study. The 9.7 km dual-purpose tunnel intended to be used as a flood control and road traffic carrier is one of the most critical underground structures in Malaysia [1]. Because of its nature in providing strategic planning in city infrastructure, it is important to consider its seismic strength. This project uses a finite element package called ABAQUS to perform dynamic analysis because it can calibrate a complicated problem experiencing large displacement, cracking, and soil-structure interaction [8]. Table I shows the material properties of soil [1]. Table II shows that seven seismic loads have been selected that pass the criteria. Fig. 1 shows the dimensions used for this project. The model was produced in four models with the difference in depth from the rock surface (0 m, 5 m, 10 m, 12.2 m).

Table 1. The Material Properties of The Soil

	Clay	Silt	Sand	Gravel
General				
Material Model	Mohr-coulomb	Mohr-coulomb	Mohr-coulomb	Mohr-coulomb
Material Behaviour	Drained	Drained	Drained	Drained
Density (Mass)	18	18	20	20
Param				
Modulus, E	9,000	8,000	90,000	120,000
Poison Ratio	0.25	0.33	0.33	0.33
Friction Angle	25	25	31	31
Dilatation Angle	0	0	0	0

Table 2. The seven seismic loads selected pass the criteria of the project

No	Earthquake	Station	Year	Mag (Mw)	Rjb (KM)	Rrup (KM)	PGA (g)	
							H	V
1	Imperial Valley, USA	Imperial Valley	1976	6.53	10.45	10.45	0.28	0.19
2	Kobe, Japan	Amagasaki	1995	6.9	11.34	11.34	0.33	0.34
3	Chi-Chi, Taiwan	TCU074	1999	7.61	0	13.46	0.6	0.28
4	Tottori, Japan	SMN001	2000	6.61	14.04	14.04	0.73	0.4
5	Duzce, Turkey	Bolu	1999	7.14	12.02	12.04	0.81	0.2
6	Iwate, Japan	MYG005	2008	6.9	10.71	13.47	0.54	0.66
7	El Mayor Cucapah, Mexico	Riito	2019	7.2	13.7	13.7	0.28	0.24

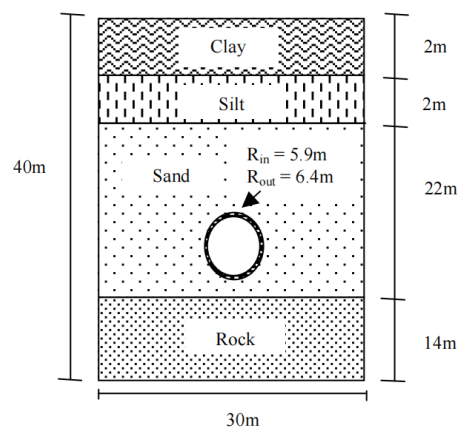


Figure 1. The SMART tunnel contains a layer of soil [1].



3. RESULT AND DISCUSSION

3.1 Natural Frequency of Structure

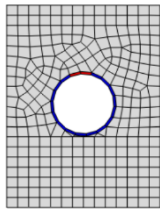
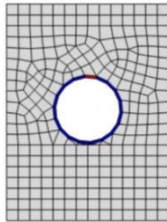
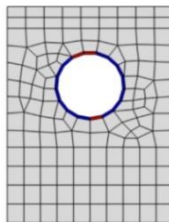
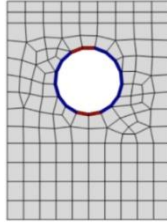
In this project a free vibration analysis has been performed before any external seismic loads have been applied, and it has been decided as to what the natural frequencies and the mode shapes of the SMART Tunnel model are. This is necessary to familiarise the dynamic nature of the tunnel-soil system and the possible weak areas and to ensure that there is a possibility of equating the seismic result with the actual realistic structural behaviours prior to the dynamic seismic work. Four samples of SMART tunnels are compared with the results available for SMART Tunnel (1).

Table 3. The Natural frequency of the structure result

Mode	Present	Free Vibration (SMART Tunnel)	Percentage Of Deviation
1	0.65	1.05	38.07
2	0.60	0.72	16.67
3	0.57	0.47	21.28
4	0.43	0.45	4.44

3.2 Limit State and Crack

According to the dynamic analysis of Abaqus with DamageT results, the crack initiation and propagation behaviour of Imperial Valley and the Chi-Chi motions were somewhat different in all 4 tunnels. Fig. 2 shows the yielding and ultimate crack pattern, which, in the Imperial Valley ground motion, the critical advancement of cracking in general, started over slow cracking and displacement compared to the Chi-Chi, Taiwan. At model 4, Imperial Valley recorded the highest displacement with 439 mm compared to Chi-Chi, Taiwan, which only recorded 335 mm. Fig. 3 to Fig. 6 show the displacement against PGA. As shown, the displacement is linear with the PGA value. Fig. 3 shows that at the low PGA of 0.05 g, the displacement ranges from 105 mm to 113 mm, and at the highest PGA of 0.4 g, it rises to 184 mm. The highest displacements are recorded under the Chi-Chi, Taiwan, earthquake, followed by Kobe and Iwate, Japan. This pattern makes sense with the characteristics of the earthquake. Chi-Chi has the highest magnitude (7.61 Mw). Fig. 4 shows that at 0.05 g, displacements start from 89 mm to 107 mm, and at 0.3 g, records like Iwate reach up to 224 mm. This occurs because the tunnel is located 5 m above the rock surface, which allows the soil layer to amplify seismic waves. In Fig. 5, at 0.05 g, displacements start high at an average of 164.3 mm for all ground motion, and at 0.20 g, most of the records, like Kobe, Chi-Chi, Duzce, Iwate, and Sierra, reach 166 mm until 170 mm. Fig. 6 shows that at 0.05 g, displacements start from 329 mm to 441 mm, and at 0.15 g, Kobe reaches up to 50% crack, which is 223 mm for the displacement.

	Model 1		Model 2	
	Imperial valley	Chi-Chi, Taiwan	Imperial valley	Chi-Chi, Taiwan
Yielding	 0.05 g S = 108 mm	 0.05 g S = 105 mm	 0.05 g S = 95mm	 0.05 g S = 95 mm



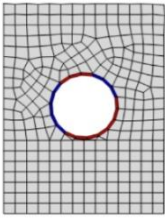
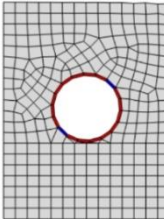
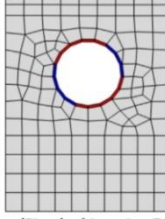
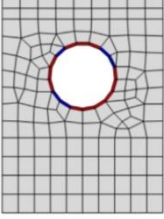
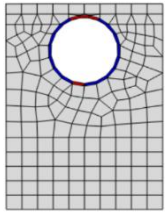
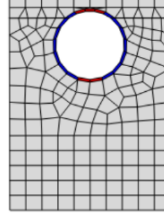
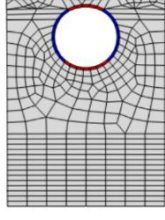
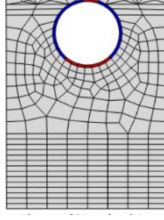
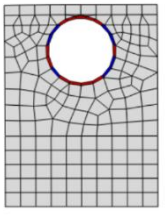
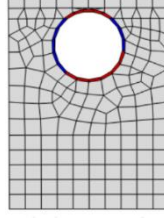
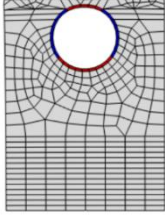
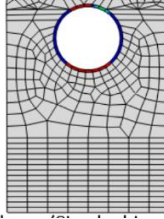
Ultimate	 0.35 g S = 173 mm	 0.05 g S = 282 mm	 0.30 g S = 202 mm	 0.20 g S = 237 mm
	Model 3		Model 4	
	Imperial valley	Chi-Chi, Taiwan	Imperial valley	Chi-Chi, Taiwan
Yielding	 0.05 g S = 169 mm	 0.05 g S = 165 mm	 0.05 g S = 329 mm	 0.05 g S = 222mm
Ultimate	 0.30 g S = 175 mm	 0.20 g S = 166 mm	 0.30 g S = 439 mm	 0.20 g S = 335 mm

Figure 2. The yielding and ultimate crack pattern.

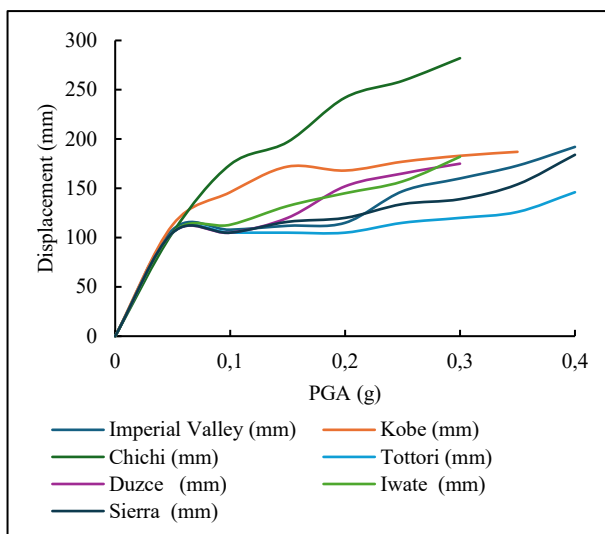


Figure 3. Incremental Dynamic Analysis Curve for Model 1

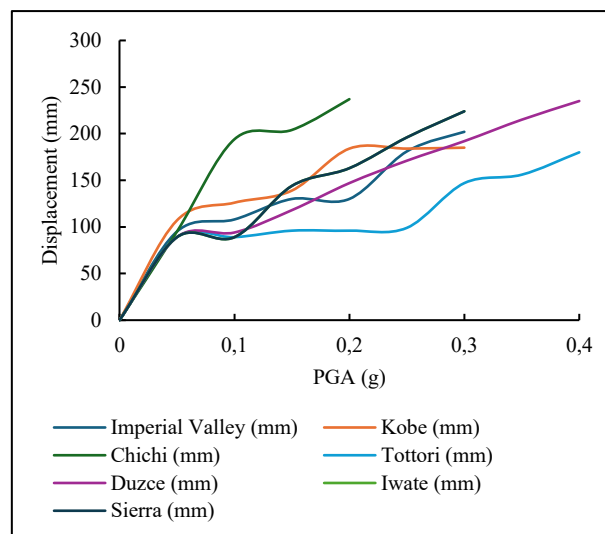


Figure 4. Incremental Dynamic Analysis Curve for Model 2

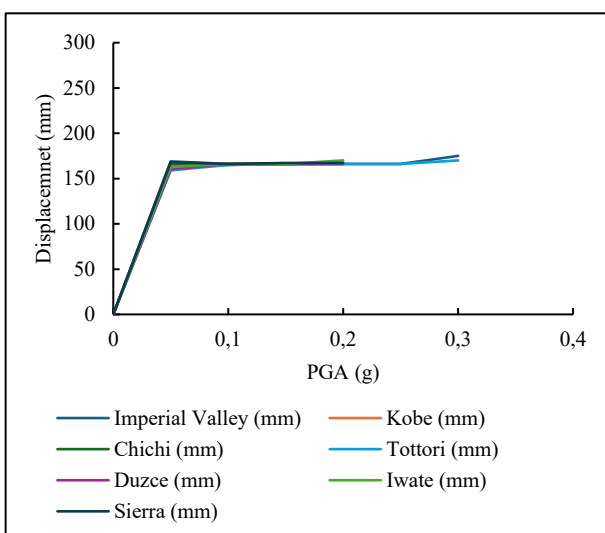


Figure 5. Incremental Dynamic Analysis Curve for Model 3

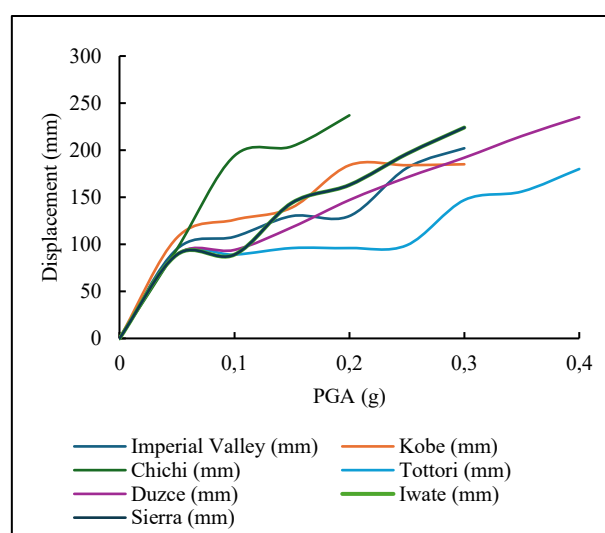


Figure 6. Incremental Dynamic Analysis Curve for Model 4

3.3 Fragility Curve

The fragility curve for the SMART Tunnel is a graphical representation that illustrates the probability of structural damage occurring under varying levels of earthquake intensity, helping to assess the tunnel's seismic vulnerability and guide risk-informed design and safety strategies.

The fragility curves in Fig. 7 to Fig. 10 illustrate the probability of tunnel collapse for Models 1 to 4 under varying seismic intensities, represented by peak ground acceleration (PGA). Each model includes two displacement thresholds: the red curve (lower displacement, onset of yielding) and the blue curve (higher displacement, near 50% crack coverage). Model 1, which is closest to the rock surface, shows a high probability of collapse at a low PGA (0.08 g) with a small displacement of 119.1 mm, indicating it is highly brittle and vulnerable to early failure. Model 2 also shows early collapse with the lowest red threshold displacement (93.3 mm), but it can withstand larger movements before reaching ultimate failure (212.4 mm).

In contrast, Model 4, which is located 12.2 m above the rock, demonstrates the highest tolerance with large displacement values (306.6 mm and 378.1 mm) and a more gradual increase in collapse probability for the blue curve, reflecting better ductility and energy absorption. Model 3 has minimal difference between yielding and ultimate displacements, indicating rapid damage progression once cracks initiate. In conclusion, Model 4 performs the best due to its ability to absorb larger displacements before failure, while Model 1 is the least effective, showing early collapse even at low seismic loads.

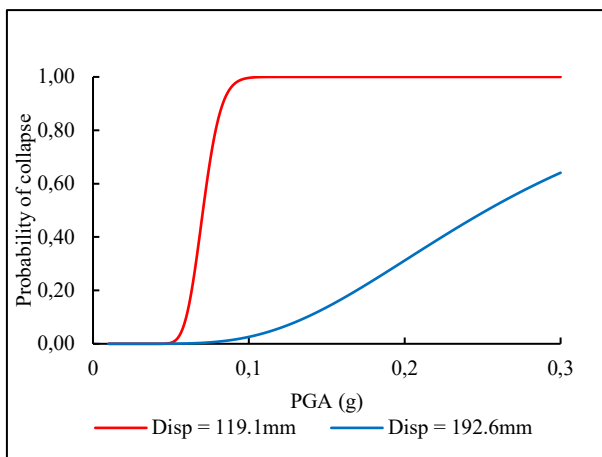


Figure 7. The fragility curve for Model 1

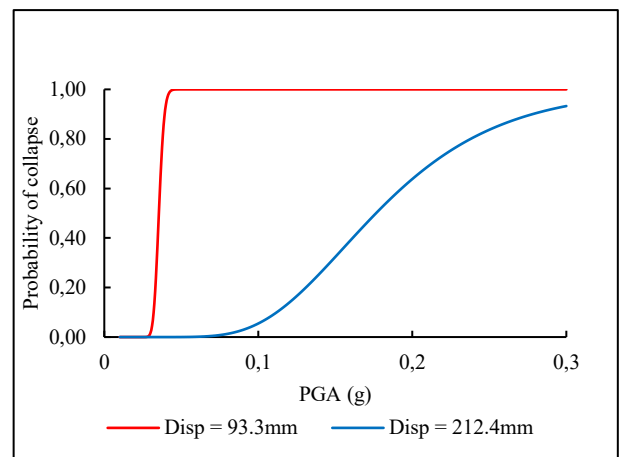


Figure 8. The fragility curve for Model 2

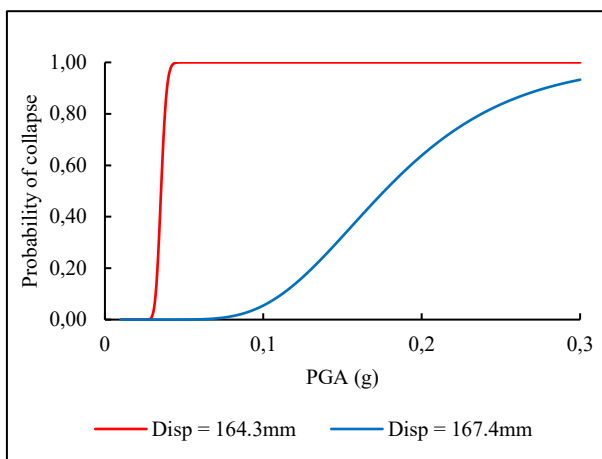


Figure 9. The fragility curve for Model 3

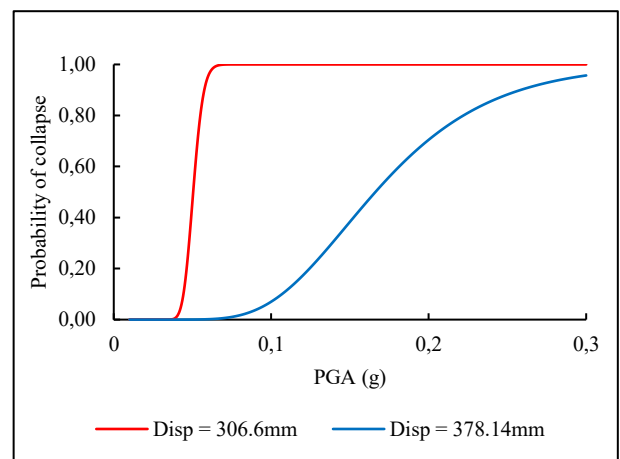


Figure 10. The fragility curve for model 4

4. CONCLUSION

The findings of this study show that the seismic performance of the SMART Tunnel is significantly influenced by the tunnel's embedment depth relative to the rock surface. Based on the fragility curves developed, Model 4, located 12.2 m above the rock, demonstrates the best seismic resilience. It exhibits the highest displacement thresholds before collapse (up to 378.1 mm) and a gradual increase in collapse probability, indicating better ductility and energy absorption. In contrast, Model 1, which lies directly on the rock surface, produces the smallest displacement (119.1 mm) yet shows a high probability of failure even at low seismic intensities (as low as 0.08 g), reflecting a more brittle behaviour and lower energy dissipation capacity.

According to [1], most severe damage tends to occur when the tunnel is positioned directly on the rock layer, as this condition prevents ovaling deformation from occurring along the tunnel lining during an earthquake. [1] also states that tunnels embedded in soft soil layers are more prone to early failure because of the amplified effects of seismic waves. In this study, however, Model 4, despite being embedded in softer soil, performs better, likely due to its greater flexibility, improved soil-structure interaction, and ability to accommodate larger movements. Therefore, it can be concluded that Model 4 is the most resilient under seismic loading, while Model 1 is the least stable, collapsing even under relatively small ground motions. These findings emphasise the critical role of tunnel placement and surrounding soil properties in designing earthquake-resistant underground structures, particularly in seismically active urban areas. Particularly in urban areas vulnerable to seismic hazards, tunnels play a crucial role. These findings directly support SDG 13 by contributing to evidence-based strategies for enhancing infrastructure resilience and adaptive capacity against earthquake-induced disasters. (5). Based on this, all objectives have been achieved, which are to investigate structural performance at varying locations under seismic loads by using nonlinear dynamic analysis, determine the limit state of the structure and lastly develop a fragility curve.



Tunnels play a crucial role. These findings directly support SDG 13 by contributing to evidence-based strategies for enhancing infrastructure resilience and adaptive capacity against earthquake-induced disasters. (5). Based on this, all objectives have been achieved, which are to investigate structural performance at varying locations under seismic loads by using nonlinear dynamic analysis, determine the limit state of the structure and lastly develop a fragility curve.

REFERENCES

- [1]. A. Adnan, M. Z. Ramli, Y. Karimi Vahed, and S. K. Che Osmi, 'Seismic Performance of Tunnel Lining under Long Distant Earthquake Effects', in *International Conference on Earthquake Engineering and Seismology (IZII-50)*, Hamburg, Germany, 2015.
- [2]. S. Anudai Anuar, N. N. M. Salleh, M. A. Rahim, and N. F. Bawadi, 'Awareness of the Seismic Effect on Existing High-rise Building in Georgetown Penang', *IOP Conference Series: Earth and Environmental Science*, vol. 1303, no. 1, 2024, doi: 10.1088/1755-1315/1303/1/012010.
- [3]. G. Awchat, A. Patil, A. More, and G. Dhanjode, 'Incremental Dynamic Analysis and Seismic Fragility Analysis of Reinforced Concrete Frame', *Civil and Environmental Engineering*, vol. 19, no. 1, 2023, doi: 10.2478/cee-2023-0039.
- [4]. M. Z. bin Abu Bakar and Z. F. binti Mohamad, 'Local government capacity for earthquake disaster risk reduction in Malaysia: Case studies in Bentong and Selayang areas', *International Journal of Disaster Risk Reduction*, vol. 97, 2023, doi: 10.1016/j.ijdr.2023.103987.
- [5]. K. Bhalla and K. Gleason, 'Effects of vehicle safety design on road traffic deaths, injuries, and public health burden in the Latin American region: a modelling study', *The Lancet Global Health*, vol. 8, no. 6, 2020, doi: 10.1016/S2214-109X(20)30102-9.
- [6]. P. Cartes, A. Chamorro, and T. Echaveguren, 'Seismic risk evaluation of highway tunnel groups', *Natural Hazards*, vol. 108, no. 2, 2021, doi: 10.1007/s11069-021-04770-1.
- [7]. M. M. Kassem, S. Beddu, J. H. Ooi, C. G. Tan, A. M. El-Maissi, and F. M. Nazri, 'Assessment of seismic building vulnerability using rapid visual screening method through web-based application for Malaysia', *Buildings*, vol. 11, no. 10, 2021, doi: 10.3390/buildings11100485.
- [8]. A. Manouchehrian and M. Cai, 'Analysis of rockburst in tunnels subjected to static and dynamic loads', *Journal of Rock Mechanics and Geotechnical Engineering*, vol. 9, no. 6, 2017, doi: 10.1016/j.jrmge.2017.07.001.
- [9]. M. Mogheisi, H. Tavakoli, and E. Peyghaleh, 'Fragility curve development of highway bridges using probabilistic evaluation (case study: Tehran City)', *Asian Journal of Civil Engineering*, vol. 24, no. 6, 2023, doi: 10.1007/s42107-023-00603-7.
- [10]. A. Moayedifar, H. R. Nejati, K. Goshtasbi, and M. Khosrotash, 'Seismic fragility and risk assessment of an unsupported tunnel using incremental dynamic analysis (IDA)', *Earthquake and Structures*, vol. 16, no. 6, 2019, doi: 10.12989/eas.2019.16.6.705.
- [11]. M. R. M. Noh, S. Rambat, I. S. B. A. Halim, and F. Ahmad, 'Seismic Risk Assessment in Malaysia: A Review', *Journal of Advanced Research in Applied Sciences and Engineering Technology*, vol. 25, no. 1, 2021, doi: 10.37934/araset.25.1.6979.
- [12]. P. J. C. Roque, R. R. Violanda, C. C. Bernido, and J. L. A. Soria, 'Earthquake occurrences in the Pacific Ring of Fire exhibit a collective stochastic memory for magnitudes, depths, and relative distances of events', *Physica A: Statistical Mechanics and its Applications*, vol. 637, 2024, doi: 10.1016/j.physa.2024.129569.
- [13]. F. Tongkul, 'An Overview of Earthquake Science in Malaysia', *ASM Science Journal*, vol. 14, 2021, doi: 10.32802/asmscj.2020.440.
- [14]. Y. Zhai, L. Zhang, B. Cui, H. Zhang, and T. Ma, 'Evolution criteria of overall damage of concrete gravity dam body and foundation under near-fault ground motion', *Structures*, vol. 43, 2022, doi: 10.1016/j.istruc.2022.06.052.
- [15]. N. S. Zulkhibri, M. I. Adiyanto, and H. A. Roslan, 'The Effect of Seismic Design on Total Cost of Structural Work for Medium Rise Apartment Building', *IOP Conference Series: Earth and Environmental Science*, vol. 1303, no. 1, 2024, doi: 10.1088/1755-1315/1303/1/012014.